Journal of Geoscience and Environment Protection, 2024, 12, 181-203
https://www.scirp.org/journal/gep
ISSN Online: 2327-4344
ISSN Print: 2327-4336

Elimination, Kinetics and Thermodynamics of Fe(II) Ions by Adsorption in Static and Dynamic Conditions on Activated Carbons in Aqueous Media

Spenseur Bouassa Mougnala[1,2*], Charly Mve Mfoumou[1,3*], Berthy Lionel Mbouiti[1,2], Pradel Tonda-Mikiela[1,3], Francis Ngoye[1], Ferdinand Evoung Evoung[1,3], Jean Aubin Ondo[4], Guy Raymond Feuya Tchouya[1,3]

[1]Laboratoire de Chimie des Milieux et des Matériaux Inorganiques (LC2MI), Département de Chimie, Université des Sciences et Techniques de Masuku (USTM), Franceville, Gabon
[2]Ecole Doctorale des Sciences Fondamentales et Appliquées (ED-SFA), LC2MI, USTM, Franceville, Gabon
[3]Département de Chimie, Faculté des Sciences (FS), USTM, Franceville, Gabon
[4]Laboratoire Pluridisciplinaire des Sciences (LAPLUS), Ecole Normale Supérieure (ENS), Libreville, Gabon
Email: *spenseurm@gmail.com, *mvefoumou@gmail.com

How to cite this paper: Mougnala, S. B., Mfoumou, C. M., Mbouiti, B. L., Tonda-Mikiela, P., Ngoye, F., Evoung, F. E., Ondo, J. A., & Tchouya, G. R. F. (2024). Elimination, Kinetics and Thermodynamics of Fe(II) Ions by Adsorption in Static and Dynamic Conditions on Activated Carbons in Aqueous Media. *Journal of Geoscience and Environment Protection, 12,* 181-203.
https://doi.org/10.4236/gep.2024.1210010

Received: July 20, 2024
Accepted: September 10, 2024
Published: October 30, 2024

Abstract

This work investigated the removal, kinetics and thermodynamics of iron(II) ions (Fe(II)) by adsorption in static and dynamic conditions in aqueous media on activated carbons (AC-i_{30min}, AC-i_{1h}, and AC-i_{24h}), prepared from palm nut shells collected in the city of Franceville to Gabon, using potassium hydroxide (KOH) as the activating agent. Results on the elimination of Fe(II) in static and dynamic adsorption on prepared activated carbons (ACs) showed that the AC-i_{24h} adsorbent has the best Fe(II) adsorption capacities at saturation (Q_{sat}). The Q_{sat} obtained on AC-i_{24h} in static and dynamic conditions (17.87 and 10.38 mg/g, respectively) were higher than those of AC-i_{30min} (13.89 and 5.54 mg/g respectively) and AC-i_{1h} (14.92 and 8.64 mg/g respectively). Moreover, the static adsorption was more effective in the removal of Fe(II) ions in aqueous media in our experimental conditions. The percentage removal (%E) of Fe(II) obtained on prepared activated carbons in static conditions was better than those obtained in dynamic conditions, especially on AC-i_{24h}, where the %E was 89.27% in static and 61.56% in dynamic. In kinetics, results showed that the pseudo-second-order kinetic model best described the adsorption mechanisms of Fe(II) on prepared activated carbons in static adsorption, with mainly of chemisorption on the solid surfaces. However, in dynamic conditions, the pseudo-first-order kinetic model was more suitable. In addition to the weak interactions between Fe(II) and the activated carbon surfaces, strong interactions

(chemisorption) were also observed. Also, thermodynamic data obtained on AC-i_{24h} in static adsorption indicated that the adsorption of Fe(II) was spontaneous and increased with temperature ($\Delta G^{\circ} < 0$) and endothermic, favoring chemisorption due to the positive value of molar enthalpy (ΔH° = 503.54 KJ/mol).

Keywords

Palm Nut Shells, Activated Carbon, Removal, Fe(II), Static and Dynamic Adsorption, Kinetics, Thermodynamics

1. Introduction

Water pollution refers to qualitative and quantitative changes in the physico-chemical and biological parameters of water (Foto et al., 2022). Human activities are the main causes of pollution in environments (water, soil, and air) due to heavy metals (Fe, Mn, Cu, Zn, Pb, As, etc.). The presence of metallic ions (Fe(II), Cu(II), Mn(II), etc.) at high concentrations in water resources resulting from industrial wastewater is a major concern for humans. The rapid growth and development of mining industries in Africa have led to continuous water pollution due to heavy metals and/or metallic ions in groundwater and rivers, often used as drinking water sources.

In Gabon, particularly in the cities of Moanda and Franceville in the Haut-Ogooué province, significant mining activity has been observed in the production of manganese (Mn) in recent years (Ndong et al., 2021). In 2019, Gabonese manganese production reached 6.1 million tons, a 17% increase from the 5.2 million tons produced in 2018 (Mve Mfoumou et al., 2022; Koumba, 2011). This same mining activity is planned to expand to the city of Makokou, in the Ogooué-Ivindo province, to exploit the iron deposits of Belinga, where iron ore reserves are estimated to exceed one billion tons (Frost-Killian et al., 2016). This increased mining activity will lead to higher concentrations of iron in the soil and surrounding water sources (Ndong et al., 2021). This could present significant health risks to the local populations and the environment. Iron, as one of the inorganic pollutants, is highly sensitive to redox reactions and easily oxidized in the environment in the presence of oxygen (Bussière et al., 2005). In its ionic form (Fe(II) or Fe(III)), iron can pose a threat to human health, with the World Health Organization (WHO) setting a limit of 0.3 mg/L for Fe(II) in drinking water (Belghiti et al., 2013; Mahamane & Guel, 2015). At high concentrations, Fe(II) can give water an unpleasant taste, lead to carcinogenic diseases, and cause benign pneumoconiosis, known as siderosis, in humans (Hosovski & Viakovic, 1990). It is therefore important to treat industrial wastewater and drinking water containing Fe(II) concentrations exceeding the limit before releasing them into the environment and distributing them in drinking water systems.

Several water treatment methods exist in industrial settings for the removal of metallic ions (Foto et al., 2022; Ndong et al., 2021; Mve Mfoumou et al., 2022; Koumba, 2011; Frost-Killian et al., 2016; Bussière et al., 2005). These methods include chemical precipitation (Abdullah et al., 2019; Patrick et al., 2015; Barakat, 2011), chemical coagulation and flocculation (Barakat, 2011; Abdullah et al., 2019; Jin et al., 2016), ion exchange techniques (Ahmed et al., 2021; Abdullah et al., 2019; Rathnayake et al., 2017), membrane filtration (Barakat, 2011), and electrochemical filtration treatments (Patrick et al., 2015). These methods, although effective at removing organic matter, are costly, energy-consuming, and require additional treatment after use. Their effectiveness against ionic species is limited due to their high solubility in water and their non-biodegradability (Yin et al., 2009). In contrast, adsorption techniques using porous solids such as activated carbons, due to their structural, textural, and chemical properties, as well as their easy preparation, are less expensive and have fewer disadvantages (Elias et al., 2021).

Several studies in the literature use adsorption techniques under static (batch) or dynamic conditions for the removal and capture of metallic ions using activated carbons (Ketsela & Animen, 2020; Elewa et al., 2023; Langama et al., 2023; Langama et al., 2021; Suksabye et al., 2008). For example, Ketsela et al. (Ketsela & Animen, 2020) demonstrated that activated carbon can be used to remove Pb(II), Co(II), and Fe(II) from aqueous solutions. Similarly, Elewa et al. (Elewa et al., 2023) studied the removal of Fe(III) and Mn(II) ions in aqueous solutions using activated carbons as adsorbents. The literature also indicates that activated carbons are prepared from carbon-rich materials using chemical activation processes (Langama et al., 2023; Mve Mfoumou et al., 2024; Balogoun et al., 2015). Furthermore, the type and concentration of activating agents (NaOH, KOH, $ZnCl_2$, H_2SO_4, etc.) influence the preparation process of activated carbons by enhancing the development of porous structures (Langama et al., 2023; Langama et al., 2021; Nunes et al., 2011). Agricultural wastes such as powders from *Azadirachta indica* leaves (Al-Aoh 2019), *Foeniculum vulgare* leaves (Bani-Atta, 2022), coconut shells, palm nut shells (Mve Mfoumou et al., 2022; Aljohani et al., 2021), and animal bones (Ezeugo et al., 2018) are among the solid materials used in the preparation of activated carbons.

The removal of heavy metals from wastewater remains a major challenge for humans. Furthermore, the methods used for their removal should be simple, effective, and cost-efficient. Since adsorption is a surface phenomenon, activated carbons with good surface properties and a large number of adsorption sites favorable for interactions between the AC surface and the metal ion, must be developed for more efficient removal. Therefore, the aim of this work was to study the elimination of Fe(II) in aqueous media by adsorption in static and dynamic conditions on activated carbons (AC) prepared from palm nut shells, using potassium hydroxide (KOH) as the chemical activating agent, in order to recover waste materials such as palm nut shells and find local solutions for treating water polluted with low concentrations of iron(II) ions. Kinetic and thermodynamic studies of

Fe(II) elimination on prepared ACs will also be carried out.

2. Experimental

2.1. Preparation of Fe(II) Solutions

A solution of Fe(II) ions at a concentration of 1000 mg/L was prepared by dissolving 4.977 g of ferrous sulfate hepta-hydrate salt ($Fe_2SO_4{\cdot}_7H_2O$, Labosi, purity: 100%) in a 1000 mL volumetric flask. For adsorption experiments in static and dynamic conditions, solutions with concentrations of 10, 50, 70, 90, 100, 150, and 200 mg/L were prepared by dilution from the 1000 mg/L Fe(II) solution.

2.2. Preparation of Activated Carbons

Palm nut shells collected in the city of Franceville in the Haut-Ogooué region of Gabon, were used as raw material for the preparation of activated carbons (ACs) using a chemical activation process (Amola et al., 2020). The palm nut shells were cleaned, ground, washed with distilled water, and then dried in an oven for 24 hours (h) at 110˚C. Afterward, 80 g of pre-treated shells were impregnated (1:1 ratio) in a 1 M potassium hydroxide solution (KOH, Acros Organics, purity: 98.5%) for 30 minutes (min), 1 h, and 24 h and then dried again for 24 h at 110˚C. After drying, the impregnated shells were calcined at 400˚C for 1 h and 30 min. with a heating rate of 5˚C/min. The ACs obtained were cooled, washed with distilled water until the pH of the residual water reached 6.5, dried for 48 h at 110˚C and sieved to obtain powdered activated carbon and granular activated carbon with particle sizes (x) of 0.04 mm < x and 0.04 mm < x < 0.1 mm, respectively (sieves: TAMISAR, Standard: AFNOR_NF-X11-501). The activated carbons obtained with impregnation times of 30 min, 1 h, and 24 h were indexed AC-i_{30min}, AC-i_{1h}, and AC-i_{24h}.

2.3. Characterization of Activated Carbons

2.3.1. Determination of Methylene Blue Number

The methylene blue number (I_{BM}) was determined using the European Chemical Industry Council method (CEFIC & EDFDLCECOCMF, 1986). 100 mg of activated carbon was mixed with 25 mL of a methylene blue solution (MB, Alp Osmose, purity: >98.5%) at 120 mg/L in a 50 mL beaker and stirred at 200 rpm for 20 min. The mixture was then filtered using a Büchner and the residual concentrations of MB were determined in colorimetry using a Thermo Electron Corporation Biomate 5 UV spectrophotometer at a wavelength λ = 664 nm. The methylene blue number (I_{BM}) is calculated using the following equation:

$$I_{BM} = \frac{\left(C_0 - C_f\right)V}{m_{AC}} \quad (1)$$

where, I_{BM} is the methylene blue number (mg·g^{-1}); C_0 is the initial concentration of methylene blue (mg·L^{-1}); C_f is the residual concentration of methylene blue

($mg \cdot L^{-1}$); m_{AC} is the activated carbon mass (g) and V is the volume of the methylene blue solution (L).

2.3.2. Determination of Iodine Number

The iodine number (I_{I_2}) was determined according to the ASTM D4607-94 method (Balogoun et al., 2015). 100, 300, and 500 mg of prepared AC were stirred in 10 mL of 1 N hydrochloric acid solution (HCl, Emsure, purity: 33%) for 30 seconds in 150 mL beakers. After cooling at room temperature, 50 mL of iodine solution of 0.02 N (I_2, Fisher Scientific) solution was added to the mixture and stirred vigorously for 30 seconds, then filtered. After filtration, 25 mL of the filtrate was titrated with 0.1 N sodium thiosulfate ($Na_2S_2O_3$, Labosi, purity: 99%) until the filtrate turned pale yellow. Then, 2 mL of a starch solution (1 g/L) was added as color indicator and titration was continued with sodium thiosulfate until the solution became colorless. The iodine number (I_{I_2}) is calculated as follows:

$$I_{I_2}\left(\mathrm{mg/g}\right) = \frac{A - \left(DF \times B \times V_{thiosulfate}\right)}{m_{AC}} \tag{2}$$

where, A is the concentration of I_2 ($mol \cdot L^{-1}$) x Molar mass of iodine ($g \cdot mol^{-1}$); B is the concentration of $Na_2S_2O_3$ ($mol \cdot L^{-1}$) x Molar Mass of Iodine ($g \cdot mol^{-1}$), DF is the dilution factor ($\frac{V_{I_2} + V_{HCl}}{V_{Filtrate}}$) and m_{AC} is activated carbon mass (g). By plotting the curve $Q_{I_2} = \int\left(C_r\right)$, the iodine number is then the value of Q_{I_2} ($mg \cdot g^{-1}$) corresponding to a residual iodine concentration of 0.04 N. The residual concentration of iodine is given by the following relationship:

$$C_r = \frac{C \cdot V_{eq}}{V} \tag{3}$$

With C_r: residual concentration of I_2 (N); C: concentration of $Na_2S_2O_3$ (N); V_{eq}: volume of $Na_2S_2O_3$ (mL) and V: volume of titrated filtrate (mL). The residual concentration of I_2 should be between 16×10^{-4} N and 8×10^{-3} N.

2.3.3. Theoretical Study of Specific Surface Areas (S_{BET})

A theoretical study of the specific surface areas was performed to estimate the specific surface areas of prepared ACs using iodine and methylene blue numbers. The method used was developed by Nunes et al. (Nunes et al., 2011). It is based on modeling the relationship between the specific surface area, the iodine and the methylene blue number using multiple regression analysis. The model used to estimate (calculate) the specific surface area is described by the following equation:

$$\begin{aligned} S\left(\mathrm{m^2/g}\right) = {} & 2.28 \times 10^2 - 1.01 \times 10^{-1} \times I_{BM} + 3 \times 10^{-1} \times I_{I_2} \\ & + 1.05 \times 10^{-4} \times I_{BM}^2 + 2 \times 10^{-4} \times I_{I_2}^2 + 9.38 \times 10^{-4} \times I_{BM} \times I_{I_2} \end{aligned} \tag{4}$$

where S is the calculated specific surface area (m^2/g), I_{BM} and I_{I_2} are respectively the methylene blue index and the iodine number (mg/g).

2.3.4. Determination of Surface Functional Groups

Surface functional groups were determined using Boehm titration (Boehm, 1966). 200 mg of activated carbon was stirred at 200 rpm in 25 mL of sodium hydroxide (NaOH, Emesure, purity: 99%), sodium bicarbonate ($NaHCO_3$, Mercek, purity: 99%), hydrochloric acid (HCl, Emsure, purity: 33%), and sodium carbonate (Na_2CO_3, Mercek, purity: 99.5%) at concentrations ranging from 0.05 to 0.1 M for 24 hours. The mixtures were filtered, and 10 mL of each filtrate was titrated with HCl or NaOH at 0.1 M to determine acidic and basic functions, respectively. The number of equivalents ($m_{eq}\cdot g^{-1}$) or concentrations ($mmol\cdot g^{-1}$) of acid or basic surface functional groups were determined by the following formula [33] [34]:

$$n\left(\text{mmol}\cdot\text{g}^{-1}\right)=\frac{C\times\left(V_b-V_s\right)\times 1000}{m_{AC}} \tag{5}$$

where C is the concentration of NaOH or HCl ($mol\cdot L^{-1}$); V_b and V_s are the equivalent volumes of the blank and sample (L), respectively; m is the mass of activated carbon (g) and 1000 is the conversion factor (mmol).

2.3.5. Determination of pH at Point of Zero Charge (pH_{pzc})

The pH at the point of zero charge (pH_{pzc}) of prepared ACs was determined according to the method described by Amola et al. (Amola et al., 2020). 40 mg of AC was placed in Erlenmeyer flasks and stirred at 200 rpm for 24 h in 20 mL of 0.1 M potassium chloride solutions (KCl, VWR Chemicals, purity: 99.5%) at different initial pH values (pH_i): 2; 5; 7 and 9. The pH of each solution was adjusted by adding either 0.1 M HCl or 0.1 M NaOH. After mixing, the solutions were left to decant, and the final pH (pH_f) was measured. The pH_{pzc} is obtained from the intersection point between the experimental curve and the theoretical curve of pH_f as a function of pH_i.

2.4. Adsorption Experiments

2.4.1. Static Adsorption

Static adsorption experiments were conducted at room temperature (24˚C - 27˚C) in five Erlenmeyer of 50 mL, each containing 20 mL of a Fe(II) ion solution at 50 mg/L and 0.05 g of prepared ACs. The mixtures were stirred at 200 rpm and the experiments were stopped at agitation times of 10, 20, 40, 60, and 80 minutes. The solutions were then filtered and a few drops of phenanthroline were added to the filtrates. The residual concentrations of Fe(II) in each Erlenmeyer flask were determined by colorimetry using a Thermo Electron Corporation Biomate 5 UV spectrophotometer at a wavelength of 512 nm based on a pre-established calibration curve for Fe(II).

The adsorption capacities at saturation (Q_{sat}) of Fe(II) for the prepared activated carbons were determined using the following expression:

$$Q_{sat}=\frac{C_0-C}{m_{AC}}\cdot V \tag{6}$$

With, Q_{sat}: adsorption capacity at saturation of activated carbon (mg/g), C_0: concentration of the solution initial of Fe(II) (mg/L), C: concentration residual of

Fe(II) (mg/L), V: Volume of the Fe(II) solution (L) and m_{AC}: mass of activated carbon (g).

Percentages of Fe(II) elimination (%E) of prepared ACs were calculated as follows:

$$\%E = \frac{C_0 - C}{C_0} \times 100 \tag{7}$$

2.4.2. Dynamic Adsorption

Dynamic adsorption experiments on a fixed-bed column of Fe(II) ions adsorption were conducted in a 55 cm long, 1.4 cm diameter glass column (Pyrex brand). The protocol and schematic of the experimental setup were described in a recent study (Mve Mfoumou et al., 2022). The experiments were carried out at room temperature (24˚C - 27˚C) using a Fe(II) solution at pH 6.5 with a concentration of 50 mg/L and a flow rate of 2 mL/min. The height of the adsorbent bed was 1 cm and the particle size ranged between $0.04 < x < 0.1$ mm. The experiments were stopped when the residual concentration (C) at the reactor outlet was equal to the concentration at the column inlet ($C/C_0 = 1$). A few drops of phenanthroline were added to solutions collected at the column outlet (every 4 minutes) in test tubes. Fe(II) concentrations in each tube (C) were determined by colorimetry using a Thermo Electron Corporation Biomate 5 UV-visible spectrophotometer at a wavelength of 512 nm.

The breakthrough curves were established by varying the ratio C/C_0 versus time (t). Exploitation of curve data $C/C_0 = \int(t)$ gives an area (A) in minutes obtained by integration according to the trapeze method (Mve Mfoumou et al., 2022; Mve Mfoumou et al., 2024):

$$A(\min) = \sum_n \frac{\left(1 - \frac{C_{t_n}}{C_0}\right) + \left(1 - \frac{C_{t_{n+1}}}{C_0}\right)}{2} \times \left(t_{n+1} - t_n\right) \tag{8}$$

where C_0 and C are the inlet and outlet concentrations (mg/L) at times t_n and t_{n+1}, respectively.

Adsorbed quantities (q_{ads}) and adsorption capacities at saturation (Q_{sat}) of Fe(II) of prepared activated carbons were calculated using the following formulas (Mve Mfoumou et al., 2022):

$$q_{ads}(\text{mg}) = D \cdot C_0 \cdot A \tag{9}$$

$$Q_{sat}(\text{mg/g}) = \frac{D \cdot C_0 \cdot A}{m_{AC}} \tag{10}$$

With D, C_0, A, and m_{AC} corresponding to the flow rate (mL/min), the concentration at the inlet of the column (mg/L), the surface area (min) corresponding to the amount of Fe(II) adsorbed and the activated carbon mass used (g) respectively.

Removal percentages of Fe(II) on prepared adsorbents (%E) were determined the following equation (Mve Mfoumou et al., 2022):

$$E(\%) = \frac{A}{t_{sat}} \times 100 \tag{11}$$

With t_{sat}: the saturation time (min).

2.5. Kinetic Studies

Adsorption kinetic studies provide information on the transfer mode of the solute from the liquid phase to the solid phase. To evaluate these parameters, the pseudo-first-order kinetic model developed by Lagergren (Belaid et al., 2011; Goertzen et al., 2010) and the pseudo-second-order kinetic model developed by Blanchard and linearized by Ho (Blanchard et al., 1984; Ho et al., 1999) were applied to the experimental data obtained from the static and dynamic adsorption of Fe(II) on prepared ACs.

The rate law of a pseudo-first-order reaction is expressed by the following equation (Belaid et al., 2011):

$$\frac{\mathrm{d}q_t}{\mathrm{d}t} = k_1 (q_e - q_t) \tag{12}$$

By integration between $t = 0$ ($q_t = 0$) and t, the following linear form is obtained:

$$\log(q_e - q_t) = \log(q_e) - \frac{k_1}{2.3} \cdot t \tag{13}$$

where q_t and q_e correspond to maximum adsorption capacities at time t and equilibrium (mg/g) respectively and k_1 is the adsorption rate constant of the pseudo-first-order kinetic model (min^{-1}).

For the pseudo-second-order kinetic model, the rate law is expressed as follows (Ho et al., 1999):

$$\frac{\mathrm{d}q}{\mathrm{d}t} = k_2 (q_e - q_t)^2 \tag{14}$$

After integration between $t = 0$ and t, and between $Q_t = 0$ and Q_t, the following linear form is obtained:

$$\frac{t}{q} = \frac{1}{k_2 \cdot q_e^2} + \frac{1}{q_e} \cdot t \tag{15}$$

where q_t and q_e correspond to maximum adsorption capacities at time t and equilibrium (mg/g) respectively and k_2 is the adsorption rate constant of the pseudo-second-order kinetic model (g/(mg·min)).

2.6. Thermodynamic Studies

The determination of thermodynamic parameters is based on the study of the Langmuir isotherm equation (Mve Zue et al., 2016). This isotherm allows for the investigation of the adsorption of molecules in the gas or liquid phase and is based on several assumptions, such as the limitation of the number of adsorption sites on the surface, the homogeneity of active sites, the occurrence of monolayer adsorption and the absence of lateral interactions between adsorbed molecules on the surface (Mve Zue et al., 2016). The Langmuir isotherm is represented by the following equation:

$$\frac{C_e}{Q_e} = \frac{1}{K_L Q_m} + \frac{C_e}{Q_m} \tag{16}$$

where Q_m is the maximum quantity of solute adsorbed (mg/g), Q_e: the quantity of solute adsorbed at equilibrium (mg/g), C_e: the residual concentration of the solute at equilibrium in the solution (mg/L), K_L: the Langmuir constant related to the adsorption energy (L/mg).

The plot of $C_e/Q_e = \int(C_e)$ gives a straight line, where the parameters $1/Q_m$ and $1/K_L Q_m$ represent the slope and intercept respectively. The Langmuir constant K_L is used to determine the Gibbs free energy of reaction (ΔG˚), which represents the degree of spontaneity of the adsorption process and indicates an energetically favorable adsorption (Mve Zue et al., 2016).

$$\Delta G° = -RT \ln K_L \tag{17}$$

where $\Delta G°$ is the Gibbs free energy (KJ/mol), R: perfect gas constant (8.314 J/mol·K) and T: the temperature (K).

The thermodynamic parameters such as entropy ($\Delta S°$) and enthalpy ($\Delta H°$) were calculated using the Van't Hoff equation (Aksu & Kabasakal, 2004; Mohan et al., 2001):

$$\ln K_d = \frac{\Delta S°}{R} - \frac{\Delta H°}{RT} \tag{18}$$

With, $\Delta H°$: the standard molar enthalpy (KJ/mol), $\Delta S°$: the standard molar entropy (J/mol·K) and K_d: the equilibrium constant.

The plot of $\ln K_d = \int(1/T)$ gives a straight line, where the parameters $\Delta H°$ and $\Delta S°$ are the slope and intercept respectively.

3. Results and Discussions

3.1. Characterization of ACs

The structural and chemical properties of prepared activated carbons (ACs) were evaluated in determining the methylene blue (I_{MB}) and iodine indices (I_{I_2}), pH of the point of zero charge (pH_{pzc}) and in quantifying the surface functional groups. Additionally, a theoretical calculation of specific surface areas was conducted.

The methylene blue number (I_{MB}) assesses the capacity of prepared ACs to adsorb or trap large-sized molecules (CEFIC & EDFDLCECOCMF, 1986). The I_{MB} results obtained for prepared ACs (**Table 1**) indicate that the methylene blue number ranges from 22.83 to 24.57 mg/g. Regardless the impregnation time of the activation agent, the I_{MB} values of prepared ACs appear similar. Moreover, these values are relatively low, indicating that prepared ACs have developed a negligible mesoporous surface volume within their pore structures (Mamane et al., 2016).

The iodine number (I_{I_2}) evaluates the capacity of ACs to adsorb or trap small molecules and thereby estimating the microporous structure of the solid (Balogoun et al., 2015). Iodine numbers obtained range from 580 to 920 mg/g (**Table 1**). Compared to values of I_{MB}, the I_{I_2} of prepared ACs are higher. It appears that the prepared adsorbents have developed micropores within their structures,

especially the AC-i_{24h} adsorbent (920 mg/g), which shows a higher I_{I_2} than AC-i_{30min} and AC-i_{1h} (580 and 560 mg/g respectively). In our experimental conditions, it seems that the longer the impregnation time of the activating agent (KOH), the better the development of the microporous structure in prepared ACs. These results are in agreement with those of Jia Guo et al. (Guo & Lua, 1999) on the textural and chemical characterization of ACs prepared from palm nut shells using KOH as the chemical activating agent. The literature also reports that the typical iodine number of ACs ranges between 500 and 1200 mg/g (Ozdemir et al., 2014). Based on the results obtained (**Table 1**), the prepared ACs exhibit iodine numbers that fall within these characteristics.

Table 1. Structural and chemical characterizations of the prepared activated carbons.

Activated carbons	$S_{BET\ cal}$ (m^2/g)	I_{MB} (mg/g)	I_{I_2} (mg/g)	pH_{pzc}	Basic functions (mmol/g)	Acidic functions (mmol/g)			
						Total	**Carboxylics**	**Lactonics**	**Phenolics**
AC-i_{30min}	480.23	24.57	580	7.40	0.55	1.55	0.850	0.225	0.475
AC-i_{1h}	468.46	22.83	560	7.60	1.40	1.05	0.150	0.125	0.775
AC-i_{24h}	691.57	23.92	920	8.00	3.05	2.40	0.550	0.025	1.825

$S_{BET\ cal}$: Calculated Specific surface area (m^2/g) using the method by Nunes et al. (Nunes et al., 2011). I_{MB}: Methylene blue number (mg/g). I_{I_2} : Iodine number (mg/g). pH_{pzc}: pH at the point of zero charge.

Results of calculated specific surface areas ($S_{BET\ cal}$) on prepared ACs are summarized in **Table 1**. The values obtained indicate that AC-i_{24h} (691.57 m^2/g) has a S_{BET} higher than AC-i_{30min} and AC-i_{1h} (480.23 and 468.46 m^2/g respectively). These results confirm the hypothesis of a greater microporous surface area on AC-i_{24h}. Similar results were observed in the works of Ubago-Pérez et al. (Ubago-Pérez et al., 2006), in studies on preparation of granular and monolithic activated carbons from olive pits using KOH as a chemical activating agent.

The pH at point of zero charge (pH_{pzc}) determines the net charge of an adsorbent (Amola et al., 2020). The net charge of activated carbons is positive below pH_{pzc} and negative above it (Amola et al., 2020).

Figure 1 shows the values of pH_{pzc} obtained on prepared ACs. The pH_{pzc} values of prepared ACs become more basic as the impregnation time of KOH increases (**Table 1**). In general, the ACs prepared using KOH activation exhibit basic pH_{pzc} values (Jawad et al., 2021; El-Hendawy, 2009). As a result, the surfaces of the prepared adsorbents will be negative or positive charged when the pH of the media is below or above pH_{pzc}.

The results of concentrations of acidic (carboxylic, lactonic, and phenolic groups) and basic surface functional groups are summarized in **Table 1**. According to the results, basic functional groups predominate on the surface of prepared ACs, except for AC-i_{30min}, which presents more acidic functional groups (**Table 1**). These results are consistent with the pH_{pzc} results of prepared ACs. Prepared adsorbents exhibit primarily basic characteristics. Similar results were observed in

the studies by Baudu et al. (Julien et al., 1998), which examined the chemical properties of activated carbons using KOH as the activating agent. However, it appears that KOH promotes the formation of basic functional groups on the surface of prepared ACs as the impregnation time increases.

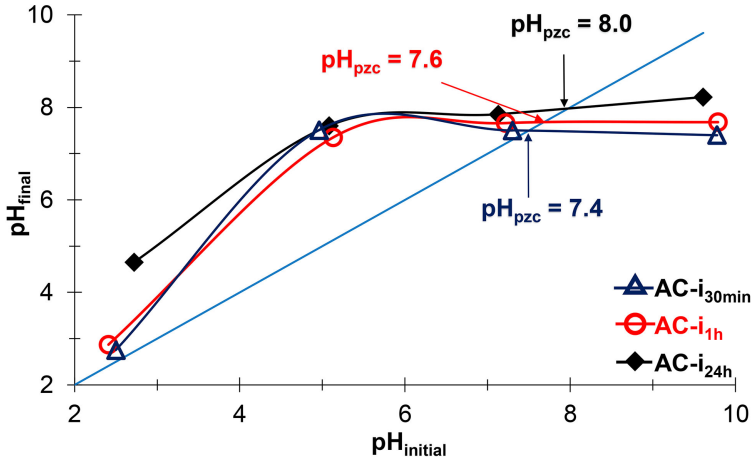

Figure 1. Determination of pH at point of zero charge (pH_{pzc}) of studied activated carbons using Boehm's titration method (Amola et al., 2020).

3.2. Static and Dynamic Adsorption of Fe(II)

Results of adsorption of Fe(II) ions in static conditions indicate that prepared adsorbents (AC-i_{30min}, AC-i_{1h} and AC-i_{24h}) have an affinity for Fe(II). Indeed, adsorption capacities at saturation (Q_{sat}) obtained on AC-i_{30min}, AC-i_{1h} and AC-i_{24h} are 13.89; 14.92 and 17.85 mg/g respectively, with removal percentages (%E) of 69.48%, 74.60%, and 89.27% respectively. The results also show that adsorption equilibria were reached after 60 min with AC-i_{24h} exhibiting the best Q_{sat} and %E values compared to AC-i_{30min} and AC-i_{1h} (Table 2). These results seem to be related to the specific surface areas (Table 1). As the S_{BET} increases, both Q_{sat} and %E improve. The adsorption and removal capacities of Fe(II) on ACs seem to be linked to the higher proportion of active sites formed due to surface modification (Rahman et al., 2023).

Table 2. Results of adsorption of Fe(II) in static and dynamic conditions on prepared adsorbents AC-i_{30min}, AC-i_{1h} and AC-i_{24h}.

Activated carbons	Static Adsorption			//	Dynamic Adsorption				
	t_{sat} (min)	Q_{sat} (mg/L)	E (%)	//	$Time_{before\ breakthrough}$ (min)	t_{sat} (min)	q_{ads} (mg)	Q_{sat} (mg/g)	E (%)
AC-i_{30min}		13.89	69.48	//	8	52	2.75	5.54	52.86
AC-i_{1h}	60	14.92	74.60	//	12	72	4.28	8.65	59.41
AC-i_{24h}		17.85	89.27	//	20	88	5.17	10.38	61.56

Compared to works of R. Sudha et al. (Sudha et al., 2007), of iron(II) ions removal on activated carbons in similar experimental conditions, capacities at

saturation (Q_{sat} = 12.15 mg/g) and the removal percentage of Fe(II) (%E = 80.40%) are lower than those obtained on AC-i_{24h} (Table 2). But those of AC-i_{24h} are lower than capacities at saturation (Q_{sat} = 57.47 mg/g) and the removal percentage of Fe(II) (%E = 99.39%) obtined in work of Alslaibi et al. (Alslaibi et al., 2014) on the kinetic and equilibrium study of the adsorption of Fe(II) on activated carbons prepared from waste of olive pits.

The results obtained demonstrate that the adsorption equilibria were reached after 60 minutes and AC-i_{24h} exhibits the highest adsorption capacity and removal percentage of Fe(II) with values of 17.85 mg/g and 89.27% respectively. These values are significantly higher than those obtained on AC-i_{30min} (13.89 mg/g and 69.48%) and AC-i_{1h} (14.92 mg/g and 74.60%). This results suggest that the higher specific surface areas (S_{BET}) contribute to the superior adsorption capacities of AC-i_{24h}. Adsorption and removal capacities of Fe(II) on ACs appear to be related to the higher proportion of active sites formed due to their surface modification (Rahman et al., 2023).

The adsorption isotherms of Fe(II) obtained on prepared activated carbons (AC-i_{30min}, AC-i_{1h}, and AC-i_{24h}) in static conditions are shown in Figure 2. The adsorbed quantities of Fe(II) increases with increasing contact time. A similar adsorption kinetic behavior is observed for all adsorbents during the first 10 min, followed by a slower adsorption rate until equilibrium is reached at around 60 minutes. A saturation time (t_{sat}) of 60 min is observed in our experimental conditions. In fact, above this value a tray is visible (Figure 2).

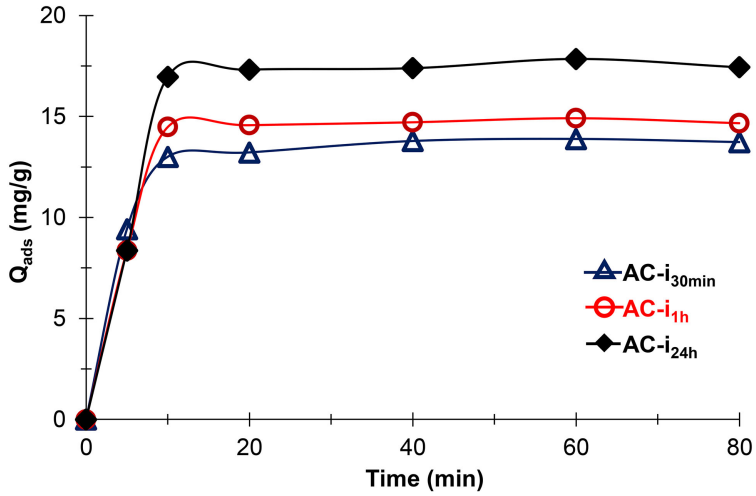

Figure 2. Adsorption isotherms of Fe(II) obtained on AC-i_{30min}, AC-i_{1h} and AC-i_{24h} at pH 6.5, stirring speed = 200 rpm and initial concentration of Fe(II) C_0 = 50 mg/L.

Results of adsorption capacities at saturation (Q_{sat}), adsorbed quantities (q_{ads}) and removal percentages (%E) obtained from dynamic adsorption experiments using a fixed-bed column for Fe(II) adsorption on AC-i_{30min}, AC-i_{1h}, and AC-i_{24h} are shown in Table 2. As in the static adsorption, the prepared ACs exhibit an

affinity for Fe(II). The prepared ACs possess adsorption sites and/or surface functional groups capable of interacting with Fe(II) in dynamic conditions. Additionally, the dynamic adsorption results (Table 2) indicate that the bed composed of AC-i_{24h} is more effective in removing Fe(II). The breakthrough and saturation times (t_{sat}), adsorbed quantities (q_{ads}), and capacities at saturation (Q_{sat}) obtained on AC-i_{24h} (20 and 88 minutes, 5.17 mg and 10.38 mg/g respectively) are higher than those obtained on AC-i_{30min} (8 and 52 minutes, 2.75 mg and 5.54 mg/g respectively) and on AC-i_{1h} (12 and 72 minutes, 4.28 mg and 8.64 mg/g respectively). These results are in agreement with those obtained in the S_{BET} (Table 1) and confirm that adsorption is indeed a surface phenomenon (Angin, 2014). Indeed, as the S_{BET} increases, the adsorbed quantities and saturation capacities improve. Dilek Angin (Angin, 2014) demonstrated that the development of specific surface areas and pore volumes plays a crucial role in the removal of metallic ions from aqueous media when using activated carbons prepared from cherry stones.

Figure 3 shows breakthrough curves of Fe(II) adsorption on prepared ACs. These curves provide information about the evolution of the ratio of the outlet (C) to inlet (C_0) concentrations of the column as a function of time. The analysis of data from breakthrough curves allows for insights into the efficiency of the bed in trapping Fe(II), based on the breakthrough and saturation times, adsorbed quantities and adsorption capacities at saturation when $C/C_0 = 1$, also on the adsorption mechanism (kinetics, type of diffusion, etc.) of Fe(II) on adsorbents studied (Mve Mfoumou et al., 2024).

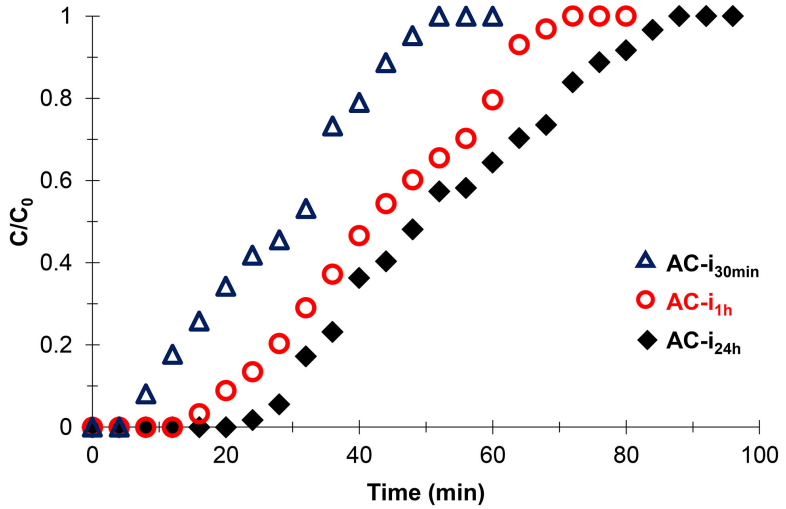

Figure 3. Breakthrough curves of Fe(II) obtained on AC-i_{30min}, AC-i_{1h} and AC-i_{24h} with a bed height (h) = 1 cm, a flow rate (D) = 2 mL/min and initial concentration of Fe(II) (C_0) = 50 mg/L.

The breakthrough curves obtained confirm that prepared ACs have an affinity with Fe(II). Breakthrough times for AC-i_{30min}, AC-i_{1h}, and AC-i_{24h} (8; 12 and 20 min respectively) and saturation times (52, 72 and 88 min respectively) confirm this. These curves indicate also a multi-step adsorption process (two types of

adsorption) of Fe(II) with different adsorption kinetics, as indicated by the varying slopes of each Fe(II) adsorption zone on prepared ACs (**Figure 3**) (Mve Mfoumou et al., 2024). The first zones, between 8 - 32, 16 - 56 and 24 - 68 min for AC-i_{30min}, AC-i_{1h} and AC-i_{24h} respectively, indicate rapid adsorption compared to the second zones (36; 60 and 72 minutes respectively until saturation) which exhibit slower adsorption rates. The steeper slopes in the first zones suggest rapid diffusion of Fe(II) containing aqueous phase to the surface or into the micropores and/or weak interactions between Fe(II) and the adsorbent surface or adsorption sites. Stronger interactions appear to occur in the second zones, as indicated by the flatter slopes (**Figure 3**) (Mve Mfoumou et al., 2024).

The results of Fe(II) adsorption indicate that the removal of Fe(II) is more effective on AC-i_{24h}, regardless of the adsorption mode (static or dynamic) as shown in **Table 2**. However, for adsorption in static conditions, the saturation capacities obtained are higher than those in dynamic conditions, regardless the adsorbents used (**Table 2**). The difference in adsorption capacities between the two modes seems to be related to the availability of adsorption sites (Li et al., 2011; Azoulay et al., 2020). In static adsorption mode, all adsorption sites (surface functional groups, pores, crevices, etc.) are utilized because the mixture is agitated and the ACs are dispersed in the solution. In contrast, in dynamic fixed-bed column adsorption, some ACs sites may not be accessible due to the overlapping of particles in the column, preventing access to all available sites (Li et al., 2011; Azoulay et al., 2020).

Thus, in our experimental conditions, static adsorption appears to be more effective in the removal of Fe(II) in aqueous media.

3.3. Kinetic Studies

Kinetic studies of Fe(II) adsorption on prepared ACs were carried out using the experimental data obtained from both static and dynamic adsorption experiments. The values of the rate constants (k), correlation coefficients (R^2), and theoretical adsorption capacities (Q_{theo}) were obtained from the plots of the linear kinetic models for pseudo-first-order and pseudo-second-order kinetics.

Figure 4 shows the linear plots for the pseudo-first-order and pseudo-second-order kinetic models applied to experimental data of the Fe(II) adsorption in static mode. According to the results, the experimental points are in agreement with the linear pseudo-second-order kinetics model (**Figure 4(b)**). Indeed, the regression coefficients (R^2) are close to unity (**Table 3**). Furthermore, the experimental (Q_{exp}) and theoretical (Q_{theo}) adsorption capacities are comparable (**Table 3**). Consequently, the kinetics of Fe(II) adsorption on prepared ACs can be described by the pseudo-second-order kinetic model, involving chemisorption, i.e. the covalent bonds between Fe(II) and the ACs on the surface of materials (Ho et al., 1999). Similar results were observed in the study of Ho et al. (Ho et al., 1999) which applied the pseudo-second-order kinetic model to the adsorption of metal ions (Cu(II), Zn(II), Pb(II), Cr(VI),and Cd(II)) on activated carbons in aqueous media.

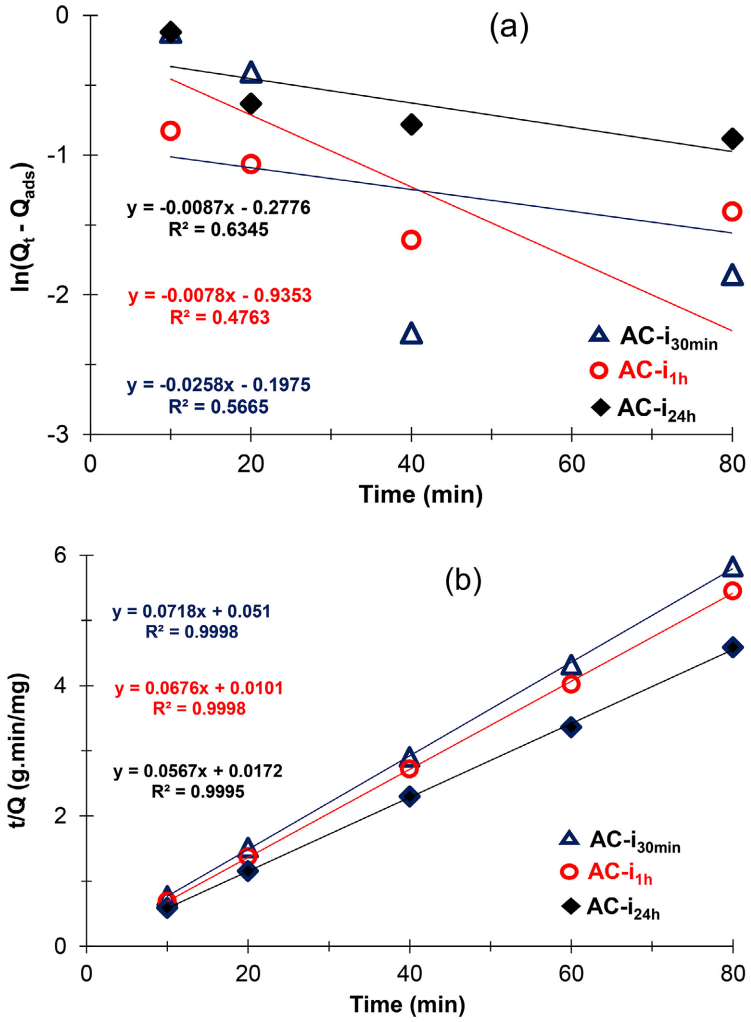

Figure 4. Linear plots of pseudo-first-order (a) and pseudo-second-order (b) kinetic models applied to the experimental data of Fe(II) adsorption in static conditions on prepared ACs.

Table 3. Parameters of linear kinetic models of pseudo-first-order and pseudo-second-order were applied to experimental data on Fe(II) adsorption in static and dynamic conditions on prepared ACs.

Activated carbons	Parameters of Fe(II) adsorption kinetics in dynamic condition							//	Parameters of Fe(II) adsorption kinetics in static condition						
	Experimental Data	Pseudo-First-Order			Pseudo-Second-Order			//	Experimental Data	Pseudo-First-Order			Pseudo-Second-Order		
	Q_{exp} (mg/g)	Q_{theo} (mg/g	$k{\cdot}10^{-4}$ (min^{-1})	R^2	Q_{theo} (mg/g)	$k{\cdot}10^{-4}$ (min^{-1})	R^2	//	Q_{exp} (mg/g)	Q_{theo} (mg/g)	$k{\cdot}10^{-4}$ (min^{-1})	R^2	Q_{theo} (mg/g)	$k{\cdot}10^{-4}$ (min^{-1})	R^2
AC-i$_{30min}$	5.54	5.06	380	0.987	8.20	480	0.992	//	13.89	0.82	44	0.026	13.93	500	0.999
AC-i$_{1h}$	8.64	8.90	450	0.980	18.25	180	0.982	//	14.92	0.55	44	0.203	14.79	4500	0.999
AC-i$_{24h}$	10.38	10.94	380	0.983	20.96	150	0.994	//	17.85	0.76	87	0.635	17.64	1900	0.999

Contrary to results of the static adsorption, in dynamic conditions the pseudo-first-order kinetic model is the model that best describes the adsorption mechanisms of Fe(II) on prepared adsorbents. Indeed, the Q_{theo} obtained are comparable

with those obtained experimentally. This is not the case for the Q_{exp} obtained with the pseudo-second-order kinetic model (Table 3). However, regardless of the model applied, the experimental points are in agreement with both models, as shown in Figure 5. Moreover, the R^2 values are close to 1 in both cases (Table 3). In dynamic fixed-bed column adsorption, both weak interactions (physisorption) and covalent bonds (chemisorption) between Fe(II) and ACs occur at the surface of the solids. These adsorption mechanisms (interactions) are due to the acidic and basic functional groups present on the surface of activated carbons (ACs). The carboxyl (-COOH) and hydroxyl (-OH) groups are those that form hydrogen bonds between Fe(II) and the ACs (Suo et al., 2020), responsible for reversible interactions (physisorption) on the surface of ACs. On the other hand, the chemisorption reactions observed are due to nitrogenous functional groups ($-NH_2$, -NH, -C=N and C-N) or Lewis bases ($-COO^-$) (Suo et al., 2020; Yang et al., 2019), which form covalent bonds or complexes with the metal ions in solution. However, reversible reactions (physisorption) are dominant. These results correspond to those of Mve Mfoumou et al. (Mve Mfoumou et al., 2024) on the study of adsorption kinetics of Cu(II) on activated carbons in aqueous media in dynamic conditions.

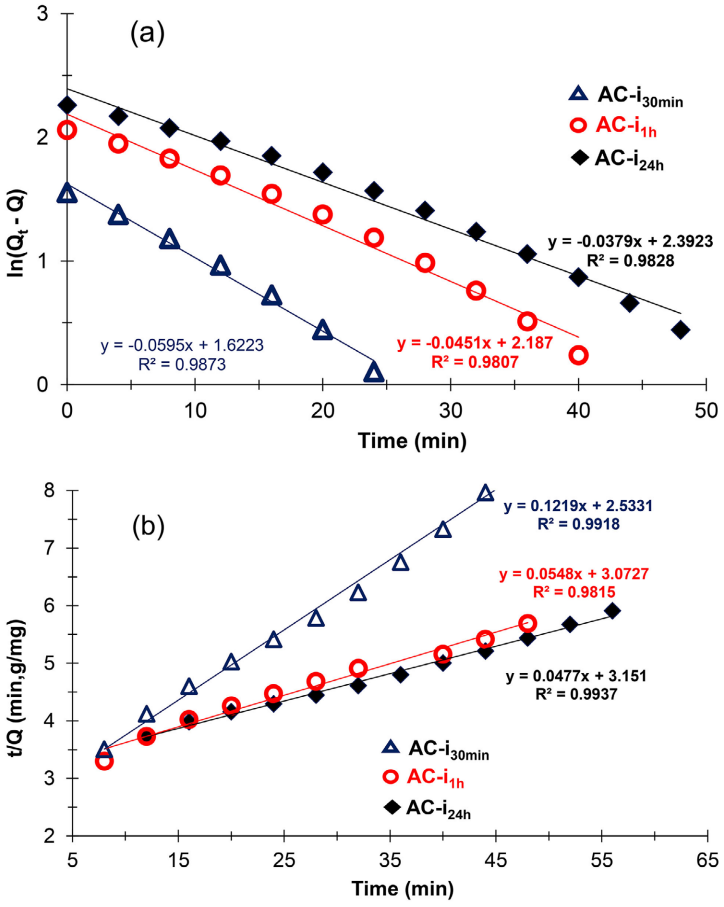

Figure 5. Linear plots of pseudo-first-order (a) and pseudo-second-order (b) kinetic models were applied to experimental data on Fe(II) adsorption in dynamic conditions on prepared ACs.

3.4. Thermodynamic Studies

The thermodynamic study of Fe(II) adsorption was carried out using data from static adsorption experiments at different temperatures (298, 333 and 373 K) and applying the Langmuir model to experimental points to determine the Langmuir constant (K_L). The study focused therefore solely on the adsorbent AC-i_{24h}, which exhibited the best surface properties and Fe(II) removal percentage in our experimental conditions.

The thermodynamic curve of the Fe(II) adsorption in static conditions on AC-i_{24h} is shown in **Figure 6** and the Langmuir parameters (Q_{sat} and K_L) as well as the thermodynamic parameters (ΔG°, ΔH° and ΔS°) are summarized in **Table 4**. The results of **Table 4** show negative values for the Gibbs free energy ($\Delta G^\circ < 0$), indicating the feasibility and spontaneity of Fe(II) adsorption on AC-i_{24h}, which becomes more spontaneous as temperature increases (Kumar & Gayathri, 2009). The results also show positive values of entropy ($\Delta S^\circ > 0$) and standard molar enthalpy ($\Delta H^\circ > 0$) with values of 7.37 J/mol·K and 503.54 KJ/mol respectively. The positive value of ΔS° reflects the affinity of AC-i_{24h} for Fe(II) and indicates an increase in randomness at the solid-solution interface during the adsorption process (Hameed et al., 2009; Thajeel et al., 2013). The positive value of ΔH° suggests that the adsorption of Fe(II) on AC-i_{24h} is endothermic, favoring chemical adsorption with the formation of covalent bonds between AC-i_{24h} and Fe(II) (Netpradit et al., 2004; Cantu et al., 2018). This result confirms the hypothesis of chemisorption at the surface of the prepared ACs, as suggested by the pseudo-second-order kinetic model.

Similar results were observed in studies by Cantu et al. (Cantu et al. 2018) and Thajeel et al. (Thajeel et al., 2013), which investigated the thermodynamic parameters of metal ion adsorption (Cu(II), Pb(II), etc.) on activated carbon adsorbents in batch adsorption.

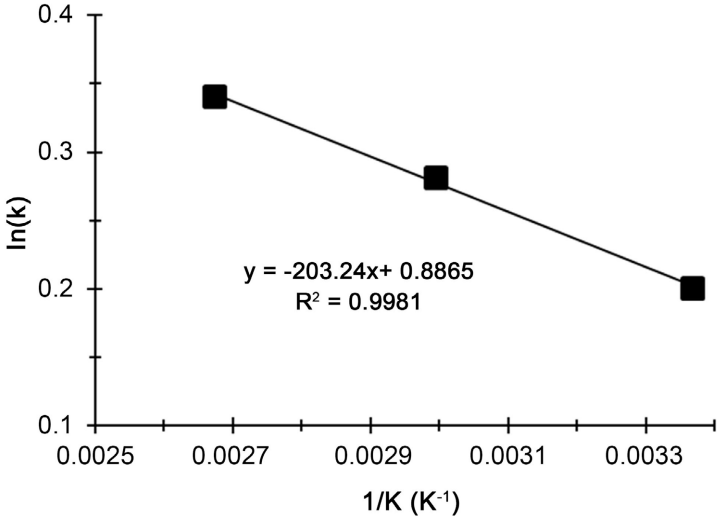

Figure 6. Thermodynamic curve of Fe(II) adsorption on AC-i_{24h} at different temperatures (298, 333 and 373 K) obtained from Van't Hoff's equation [39] [40].

Table 4. Parameters of Langmuir and thermodynamic for Fe(II) adsorption on AC-i_{24h}.

Activated carbon	Températures (K)	Langmuir Parameters		Thermodynamic Parameters			
		Q_{sat} (mg/g)	K_L (L/mg)	ΔG° (KJ/mol)	ΔH° (KJ/mol)	ΔS° (J/mol·K)	R^2
AC-i_{24h}	298	17.85	1.22	−0.498	503.54	7.37	0.998
	333	18.01	1.33	−0.779			
	373	17.99	1.41	−1.058			

4. Conclusion

The objective of this work was to study the removal of iron(II) ions (Fe(II)) through static and dynamic adsorption on a fixed-bed column in aqueous media using activated carbons (AC-i_{30min}, AC-i_{1h} and AC-i_{24h}). These activated carbons (ACs) were prepared from palm nut shells collected in the city of Franceville in Gabon, using potassium hydroxide (KOH) as the activation agent. Additionally, kinetic and thermodynamic studies of Fe(II) adsorption were conducted.

Structural and chemical characterizations of prepared activated carbons (ACs) showed that the prepared ACs have calculated specific surface areas (S_{BETcal}) ranging from 468 to 692 m^2/g, predominantly basic surface functional groups and mainly microporous structures with a basic character. However, AC-i_{24h} exhibited superior values of S_{BETcal} (691.51 m^2/g), iodine number (I_{I_2} = 920 mg/g), surface functional group concentration (C = 3.05 mmol/g) and a pH at point of zero charge (pH_{pzc} = 8) compared to AC-i_{30min} and AC-i_{1h}.

Studies on the removal of Fe(II) ions through static and dynamic adsorption on prepared ACs showed that AC-i_{24h} had the best adsorption capacities. Indeed, the saturation adsorption capacities (Q_{sat}) obtained on AC-i_{24h} in static and dynamic conditions (17.87 and 10.38 mg/g respectively) were higher than those obtained on AC-i_{30min} (13.89 and 5.54 mg/g respectively) and AC-i_{1h} (14.92 and 8.64 mg/g respectively). Furthermore, the adsorption in static conditions was more effective in removing Fe(II) in aqueous media in our experimental conditions. Removal percentages (%E) of Fe(II) of prepared ACs in static conditions were better than those in dynamic conditions, particularly for AC-i_{24h}, where the %E was 89.27% in static adsorption and 61.56% in dynamic adsorption.

Kinetic studies showed that the pseudo-second-order kinetic model best describes the mechanisms of Fe(II) adsorption on prepared ACs in static conditions with chemisorption primarily occurring on surfaces of prepared ACs. However, in dynamic conditions, the pseudo-first-order kinetic model was more suitable. In addition to weak, predominant interactions between Fe(II) and the surfaces of ACs, strong interactions (chemisorption) also occurred. Also, thermodynamic data obtained for AC-i_{24h} in static adsorption indicated that the adsorption of Fe(II) was spontaneous and increased with temperature ($\Delta G^\circ < 0$), that the process was endothermic, favoring chemisorption due to the positive value of the molar enthalpy (ΔH° = 503.54 KJ/mol).

Declaration of Conflicting Interests

The authors do not work for, advise, own shares in, or receive funds from any organization that might benefit from this article and have declared no affiliation other than their research organizations.

Conflicts of Interest

The authors declare no conflicts of interest regarding the publication of this paper.

References

Abdullah, N., Yusof, N., Lau, W. J., Jaafar, J., & Ismail, A. F. (2019). Recent Trends of Heavy Metal Removal from Water/wastewater by Membrane Technologies. *Journal of Industrial and Engineering Chemistry, 76,* 17-38. https://doi.org/10.1016/j.jiec.2019.03.029

Ahmed, S. F., Mofijur, M., Nuzhat, S., Chowdhury, A. T., Rafa, N., Uddin, M. A. et al. (2021). Recent Developments in Physical, Biological, Chemical, and Hybrid Treatment Techniques for Removing Emerging Contaminants from Wastewater. *Journal of Hazardous Materials, 416,* Article ID: 125912. https://doi.org/10.1016/j.jhazmat.2021.125912

Aksu, Z., & Kabasakal, E. (2004). Batch Adsorption of 2, 4-Dichlorophenoxy-Acetic Acid (2, 4-D) from Aqueous Solution by Granular Activated Carbon. *Separation and Purification Technology, 35,* 223-240. https://doi.org/10.1016/s1383-5866(03)00144-8

Al-Aoh, H. A. (2019). Equilibrium, Thermodynamic and Kinetic Study for Potassium Permanganate Adsorption by Neem Leaves Powder. *Desalination and Water Treatment, 170,* 101-110. https://doi.org/10.5004/dwt.2019.24905

Aljohani, M. M. H., & AL-Aoh, H. A. (2021). Adsorptive Removal of Permanganate Anions from Synthetic Wastewater Using Copper Sulfide Nanoparticles. *Materials Research Express, 8,* Article ID: 035012. https://doi.org/10.1088/2053-1591/abef40

Alslaibi, T. M., Abustan, I., Ahmad, M. A., & Foul, A. A. (2014). Kinetics and Equilibrium Adsorption of Iron (II), Lead (II), and Copper (II) Onto Activated Carbon Prepared from Olive Stone Waste. *Desalination and Water Treatment, 52,* 7887-7897. https://doi.org/10.1080/19443994.2013.833875

Amola, L. A., Kamgaing, T., Tchuifon, D. R. T., Atemkeng, C. D., & Anagho, S. G. (2020). Activated Carbons Based on Shea Nut Shells (*Vitellaria paradoxa*): Optimization of Preparation by Chemical Means Using Response Surface Methodology and Physicochemical Characterization. *Journal of Materials Science and Chemical Engineering, 8,* 53-72. https://doi.org/10.4236/msce.2020.88006

Angin, D. (2014). Production and Characterization of Activated Carbon from Sour Cherry Stones by Zinc Chloride. *Fuel, 115,* 804-811. https://doi.org/10.1016/j.fuel.2013.04.060

Azoulay, K., Bencheikh, I., Moufti, A., Dahchour, A., Mabrouki, J., & El Hajjaji, S. (2020). Comparative Study between Static and Dynamic Adsorption Efficiency of Dyes by the Mixture of Palm Waste Using the Central Composite Design. *Chemical Data Collections, 27,* Article ID: 100385. https://doi.org/10.1016/j.cdc.2020.100385

Balogoun, C., Bawa, M., Osseni, S., & Aina, M. (2015). Préparation des charbons actifs par voie chimique à l'acide phosphorique à base de coque de noix de coco. *International Journal of Biological and Chemical Sciences, 9,* 563-580. https://doi.org/10.4314/ijbcs.v9i1.48

Bani-Atta, S. A. (2022). Potassium Permanganate Dye Removal from Synthetic Wastewater

Using a Novel, Low-Cost Adsorbent, Modified from the Powder of Foeniculum Vulgare Seeds. *Scientific Reports, 12,* Article No. 4547. https://doi.org/10.1038/s41598-022-08543-z

Barakat, M. A. (2011). New Trends in Removing Heavy Metals from Industrial Wastewater. *Arabian Journal of Chemistry, 4,* 361-377. https://doi.org/10.1016/j.arabjc.2010.07.019

Belaid, K. D., & Kacha, S. (2011). Étude cinétique et thermodynamique de l'adsorption d'un colorant basique sur la sciure de bois. *Revue des sciences de l'eau, 24,* 131-144. https://doi.org/10.7202/1006107ar

Belghiti, M. L., Chahlaoui, A., & Bengoumi, D. (2013). Study of Physical Quality-Chemical and Bacteriological of Groundwater from the Plio-Quaternary Aquifer in the Meknes Region (Morocco). *LARHYSS Journal, 1112,* 21-36.

Blanchard, G., Maunaye, M., & Martin, G. (1984). Removal of Heavy Metals from Waters by Means of Natural Zeolites. *Water Research, 18,* 1501-1507. https://doi.org/10.1016/0043-1354(84)90124-6

Boehm, H. P. (1966). Chemical Identification of Surface Groups. *Advances in Catalysis, 16,* 179-274. https://doi.org/10.1016/s0360-0564(08)60354-5

Bussière, B., Aubertin, M., Zagury, G. J., Potvin, R. and Benzaazoua, M. (2005). Principaux défis et pistes de solution pour la restauration des aires d'entreposage de rejets miniers abandonnées. In *Proceedings of the Symposium* (pp. 1-29). Academia Education.

Cantu, J., Gonzalez, D. F., Cantu, Y., Eubanks, T. M., & Parsons, J. G. (2018). Thermodynamic and Kinetic Study of the Removal of Cu^{2+} and Pb^{2+} Ions from Aqueous Solution Using Fe_7S_8 Nanomaterial. *Microchemical Journal, 140,* 80-86. https://doi.org/10.1016/j.microc.2018.04.003

CEFIC & EDFDLCECOCMF (European Council of Chemical Manufacturers Federation/European Chemical Industry Council) (1986). *Test Methods for Activated Carbon* (pp. 9-43).

Elewa, A. M., Amer, A. A., Attallah, M. F., Gad, H. A., Al-Ahmed, Z. A. M., & Ahmed, I. A. (2023). Chemically Activated Carbon Based on Biomass for Adsorption of Fe(III) and Mn(II) Ions from Aqueous Solution. *Materials, 16,* Article 1251. https://doi.org/10.3390/ma16031251

El-Hendawy, A. A. (2009). An Insight into the KOH Activation Mechanism through the Production of Microporous Activated Carbon for the Removal of Pb^{2+} Cations. *Applied Surface Science, 255,* 3723-3730. https://doi.org/10.1016/j.apsusc.2008.10.034

Elias, M. A., Hadibarata, T., & Sathishkumar, P. (2021). Modified Oil Palm Industry Solid Waste as a Potential Adsorbent for Lead Removal. *Environmental Chemistry and Ecotoxicology, 3,* 1-7. https://doi.org/10.1016/j.enceco.2020.10.003

Ezeugo, D. J. (2018). Removal of Potassium Permanganate from Aqueous Solution by Adsorption onto Activated Carbon Prepared from Animal Bone and Corn Cob. *Equatorial Journal of Engineering, No. 2018,* 29-36.

Foto, E., Allahdin, O., Biteman, O., & Poumaye, N. (2022). Assessment of Water Contamination by Metallic Trace Elements at Mining Sites: The Case of the Ouham River in the Central African Republic. *American Journal of Environmental Protection, 10,* 47-56.

Frost-Killian, S., Master, S., Viljoen, R. P., & Wilson, M. G. C. (2016). The Great Mineral Fields of Africa Introduction. *Episodes, 39,* 85-103. https://doi.org/10.18814/epiiugs/2016/v39i2/95770

Goertzen, S. L., Thériault, K. D., Oickle, A. M., Tarasuk, A. C., & Andreas, H. A. (2010). Standardization of the Boehm Titration. Part I. CO_2 Expulsion and Endpoint Determination. *Carbon, 48,* 1252-1261. https://doi.org/10.1016/j.carbon.2009.11.050

Guo, J., & Lua, A. C. (1999). Textural and Chemical Characterisations of Activated Carbon Prepared from Oil-Palm Stone with H_2SO_4 and KOH Impregnation. *Microporous and Mesoporous Materials, 32,* 111-117. https://doi.org/10.1016/s1387-1811(99)00096-7

Hameed, B. H., Ahmad, A. A., & Aziz, N. (2009). Adsorption of Reactive Dye on Palm-Oil Industry Waste: Equilibrium, Kinetic and Thermodynamic Studies. *Desalination, 247,* 551-560. https://doi.org/10.1016/j.desal.2008.08.005

Ho, Y. S., & McKay, G. (1999). Pseudo-Second Order Model for Sorption Processes. *Process Biochemistry, 34,* 451-465. https://doi.org/10.1016/s0032-9592(98)00112-5

Hosovski, E., & Viakovic, A. (1990). Kidney Injuries Due to Inhalation of Copper Dust and Fumes. In *Abstracts 23 rd International Congress on Occupational Health-Montréal* (pp. 305).

Jawad, A. H., Saud Abdulhameed, A., Wilson, L. D., Syed-Hassan, S. S. A., ALOthman, Z. A., & Rizwan Khan, M. (2021). High Surface Area and Mesoporous Activated Carbon from Koh-Activated Dragon Fruit Peels for Methylene Blue Dye Adsorption: Optimization and Mechanism Study. *Chinese Journal of Chemical Engineering, 32,* 281-290. https://doi.org/10.1016/j.cjche.2020.09.070

Jin, W., Du, H., Zheng, S., & Zhang, Y. (2016). Electrochemical Processes for the Environmental Remediation of Toxic Cr(VI): A Review. *Electrochimica Acta, 191,* 1044-1055. https://doi.org/10.1016/j.electacta.2016.01.130

Julien, F., Baudu, M., & Mazet, M. (1998). Relationship between Chemical and Physical Surface Properties of Activated Carbon. *Water Research, 32,* 3414-3424. https://doi.org/10.1016/s0043-1354(98)00109-2

Ketsela, G., & Animen, Z. (2020). Adsorption of Lead (II), Cobalt (II) and Iron (II) from Aqueous Solution by Activated Carbon Prepared from White Lupine (GIBITO) HSUK. *Journal of Thermodynamics and Catalysis, 11,* 1-8.

Koumba, C. (2011). La gestion et l'exploitation des ressources naturelles au Gabon: Vers une réorganisation spatiale des activités productives. *Les Cahiers d'Outre-Mer, 64,* 507-521. https://doi.org/10.4000/com.6399

Kumar, P. S., & Gayathri, R. (2009). Adsorption of Pb^{2+} Ions from Aqueous Solutions onto Bael Tree Leaf Powder: Isotherms, Kinetics and Thermodynamics Study. *Journal of Engineering Science and Technology, 4,* 381-399.

Langama, P. L. M., Anguile, J. J., Bissielou, C., Bouraïma, A., Ndong, A. N. M. M., Kouotou, D. et al. (2023). Preparation and Characterization of Activated Carbons from Asparagus Palm (*Laccosperma robustum*) Bark by Chemical Activation with H_3PO_4 and KOH. *American Journal of Analytical Chemistry, 14,* 55-71. https://doi.org/10.4236/ajac.2023.142004

Langama, P. L. M., Anguile, J. J., Ndong, A. N. M. M., Bouraima, A., & Bissielou, C. (2021). Adsorption of Copper (II) Ions in Aqueous Solution by a Natural Mouka Smectite and an Activated Carbon Prepared from Kola Nut Shells by Chemical Activation with Zinc Chloride ($ZnCl_2$). *Open Journal of Inorganic Chemistry, 11,* 131-144. https://doi.org/10.4236/ojic.2021.114009

Li, W., Yue, Q., Tu, P., Ma, Z., Gao, B., Li, J. et al. (2011). Adsorption Characteristics of Dyes in Columns of Activated Carbon Prepared from Paper Mill Sewage Sludge. *Chemical Engineering Journal, 178,* 197-203. https://doi.org/10.1016/j.cej.2011.10.049

Mahamane, A. A., & Guel, B. (2015). Caractérisations physico-chimiques des eaux souterraines de la localité de Yamtenga (Burkina Faso). *International Journal of Biological and Chemical Sciences, 9,* 517-533. https://doi.org/10.4314/ijbcs.v9i1.44

Mamane, O. S., Zanguina, A., & Daou, I. (2016). Preparation and Characterization of

Activated Carbons Based on Core Shells of Balanites Eagyptiaca and Zizyphus Mauritiana. *Journal of the West African Society of Chemistry, 41,* 59-67.

Mohan, D., Gupta, V. K., Srivastava, S. K., & Chander, S. (2001). Kinetics of Mercury Adsorption from Wastewater Using Activated Carbon Derived from Fertilizer Waste. *Colloids and Surfaces A: Physicochemical and Engineering Aspects, 177,* 169-181. https://doi.org/10.1016/s0927-7757(00)00669-5

Mve Mfoumou, C., Tonda-Mikiela, P., Ngoye, F., Berthy Lionel, M., Mougnala Spenseur, B., Sachse, A. et al. (2022). Dynamic Adsorption on Fixed-Bed Column of Manganese Oxoanions (MnO_4^-) in Aqueous Media on Activated Carbon Prepared from Palm Nut Shells. *Journal of Environment Pollution and Human Health, 10,* 58-70. https://doi.org/10.12691/jephh-10-2-4

Mve Mfoumou, C., Tonda-Mikiéla, P., Ngoye, F., Bouassa Mougnala, S., Mbouiti, B. L., & Feuya Tchouya, G. R. (2024). Removal and Adsorption Kinetics of Copper(II) Ions from Aqueous Media on Activated Carbon in Dynamic Adsorption on a Fixed-Bed Column. *Comptes Rendus Chimie, 27,* 141-151. https://doi.org/10.5802/crchim.285

Mve Zue, M., Makani, T., & Eba, F. (2016). Removal of Mn(II) from Aqueous Solutions by Activated Carbons Prepared from Coula Edulis Nut Shell. *Journal of Environmental Science and Technology, 9,* 226-237. https://doi.org/10.3923/jest.2016.226.237

Ndong, A. N. M. M., Bouraïma, A., Bissielou, C., Anguile, J., & Makani, T. (2021). Chemical Composition Assessment by Wavelength Dispersive X-Ray Fluorescence of Agricultural Soils in the Mining Town of Moanda, Gabon. *Journal of Agricultural Chemistry and Environment, 10,* 345-358. https://doi.org/10.4236/jacen.2021.103022

Netpradit, S., Thiravetyan, P., & Towprayoon, S. (2004). Adsorption of Three Azo Reactive Dyes by Metal Hydroxide Sludge: Effect of Temperature, Ph, and Electrolytes. *Journal of Colloid and Interface Science, 270,* 255-261. https://doi.org/10.1016/j.jcis.2003.08.073

Nunes, C. A., & Guerreiro, M. C. (2011). Estimation of Surface Area and Pore Volume of Activated Carbons by Methylene Blue and Iodine Numbers. *Química Nova, 34,* 472-476. https://doi.org/10.1590/s0100-40422011000300020

Ozdemir, I., Şahin, M., Orhan, R., & Erdem, M. (2014). Preparation and Characterization of Activated Carbon from Grape Stalk by Zinc Chloride Activation. *Fuel Processing Technology, 125,* 200-206. https://doi.org/10.1016/j.fuproc.2014.04.002

Patrick, A. G., N'guadi Blaise, A., Kouamé, D. B., Ouattara, K. D., Kgildas, G., & Albert, T. (2015). Butyl Paraben Adsorption on Coal Based on Low Cost of Coconut Shells from Ivory Coast. *International Journal of Innovation and Scientific Research, 13,* 530-541.

Rahman, U. U., Humayun, M., Khan, A., Farooq, S., Sadiq, M., Bououdina, M. et al. (2023). Thermo-Chemical Modification of Cellulose for the Adsorptive Removal of Titan Yellow from Wastewater. *Molecules, 28,* Article 3955. https://doi.org/10.3390/molecules28093955

Rathnayake, S. I., Martens, W. N., Xi, Y., Frost, R. L., & Ayoko, G. A. (2017). Remediation of Cr (VI) by Inorganic-Organic Clay. *Journal of Colloid and Interface Science, 490,* 163-173. https://doi.org/10.1016/j.jcis.2016.11.070

Sudha, R., Kalpana, K., Rajachandrasekar, T., & Arivoli, S. (2007). Comparative Study on the Adsorption Kinetics and Thermodynamics of Metal Ions onto Acid Activated Low Cost Pandanus Carbon. *Journal of Chemistry, 4,* 238-254. https://doi.org/10.1155/2007/304305

Suksabye, P., Thiravetyan, P., & Nakbanpote, W. (2008). Column Study of Chromium(vi) Adsorption from Electroplating Industry by Coconut Coir Pith. *Journal of Hazardous Materials, 160,* 56-62. https://doi.org/10.1016/j.jhazmat.2008.02.083

Suo, C., Du, K., Yuan, R., Chen, H., Wang, F., & Zhou, B. (2020). Adsorption Study of Heavy Metal Ions from Aqueous Solution by Activated Carbon in Single and Mixed System. *Desalination and Water Treatment, 183,* 315-324. https://doi.org/10.5004/dwt.2020.25236

Thajeel, A. (2013). Technology, Isotherm, Kinetic and Thermodynamic of Adsorption of Heavy Metal Ions Onto Local Activated Carbon. *Aquatic Science and Technology, 1,* 53-77.

Ubago-Pérez, R., Carrasco-Marín, F., Fairén-Jiménez, D., & Moreno-Castilla, C. (2006). Granular and Monolithic Activated Carbons from Koh-Activation of Olive Stones. *Microporous and Mesoporous Materials, 92,* 64-70. https://doi.org/10.1016/j.micromeso.2006.01.002

Yang, X., Wan, Y., Zheng, Y., He, F., Yu, Z., Huang, J. et al. (2019). Surface Functional Groups of Carbon-Based Adsorbents and Their Roles in the Removal of Heavy Metals from Aqueous Solutions: A Critical Review. *Chemical Engineering Journal, 366,* 608-621. https://doi.org/10.1016/j.cej.2019.02.119

Yin, C. Y., Aroua, M. K., & Daud, W. M. A. W. (2009). Fixed-bed Adsorption of Metal Ions from Aqueous Solution on Polyethyleneimine-Impregnated Palm Shell Activated Carbon. *Chemical Engineering Journal, 148,* 8-14. https://doi.org/10.1016/j.cej.2008.07.032